

OLIVINE EXPOSURES IN THE SLOPES OF THE GRUITHUISEN DOMES. Z. M. Vig¹, J. M. Sunshine¹, K. L. Donaldson Hanna² and the Lunar-VISE Team, ¹University of Maryland, College Park, MD, USA (zvig@umd.edu), ²University of Central Florida, Orlando, FL, USA.

Introduction: Unexpectedly, an olivine-rich material has been detected using visible to near-infrared (VNIR) spectroscopy in the steep slopes of all three domes that make up Mons Gruithuisen—hereafter referred to as the Gruithuisen Domes. The domes were originally recognized by their distinct “red” spectral slope [1] and subsequent studies have provided evidence for VNIR spectral variability [2, 3, 4]. In addition, the position of the infrared Christiansen Feature on the domes, which is sensitive to silica polymerization [5] and thus bulk SiO₂ content, suggests that the domes are highly silicic [6], implying the existence of evolved magmatic compositions on the Moon. Given the stark differences in bulk H₂O content and tectonic environment between the Earth and the Moon, the origin of lunar evolved compositions remains enigmatic. Investigating these newly detected olivine-rich materials may help discriminate between the three hypothesized formation mechanisms for the domes: (1) silicate liquid immiscibility (SLI) [7], (2) extensive fractional crystallization with no immiscibility [8], or (3) remelting of crustal material via basaltic underplating [9]. In particular, the olivine-rich material could provide evidence for a significant mafic component to the eruptive sequence of the domes, which would lower the volume of silicic material required to produce the dome structures. By mapping this mafic material, this study will also provide compositional context information for the upcoming Lunar Vulkan Imaging and Spectroscopy Explorer (Lunar-VISE) that will obtain in-situ VNIR images at a sub-cm scale over a ~1 km rover traverse of the Gamma Dome [10].

Dataset Description: To investigate the geologic setting and composition of the olivine-rich material, we use a variety of spectral datasets including: Two modes of the Moon Mineralogy Mapper (M³) (global mode, 140m/pixel, 85 bands; targeted mode,

70m/pixel, 254 bands), the Kaguya Spectral Profiler (SP, ~250m point spectrometer, 296 bands) and the Kaguya Multiband Imager (MI, 62m/pixel, 7 bands). To improve its photometric correction, we reprocessed the M³ data from radiance (L1) using a new 2 m LROC NAC DEM [10]. In addition, we utilized high resolution NAC images to investigate the morphology of the steep slopes.

Olivine Detection: Based on the presence of a broad, 1 μ m absorption, olivine-rich material is detected in the steep slopes of all three Gruithuisen Domes (Gamma, Delta and Northwest). **Fig. 1a** shows the results of spectral mixture analysis [11] using the two acquisition modes of M³. The “olivine” endmember is an in-scene spectrum rather than a lab spectrum of known composition, so the abundance maps of **Fig. 1a** show the abundance of a mixture of olivine plus other background material.

Fig. 1b shows areally averaged spectra from select regions of interest (ROI) from within **Fig. 1a**. The 1 μ m olivine absorptions at each locality are well above the noise threshold with absorption depths of ~6-8%, similar to those of the pyroxene absorption commonly seen in weathered mare basalts. Precise mineralogical composition of the olivine-rich spectra is currently under investigation.

Incidence Angle Dependence: Multiple hyperspectral datasets exist over the Gruithuisen Domes at drastically different viewing geometries. This has allowed us to identify a strong correlation between the detection of olivine-rich material and local solar incidence angle. This correlation is shown spatially in **Fig. 1** and explicitly in **Fig. 2a**. Analysis of spectral characteristics suggests that neither instrumental noise nor photometric effects are responsible for this relationship, so the physical setting of the olivine-rich exposures was investigated as a possible cause.

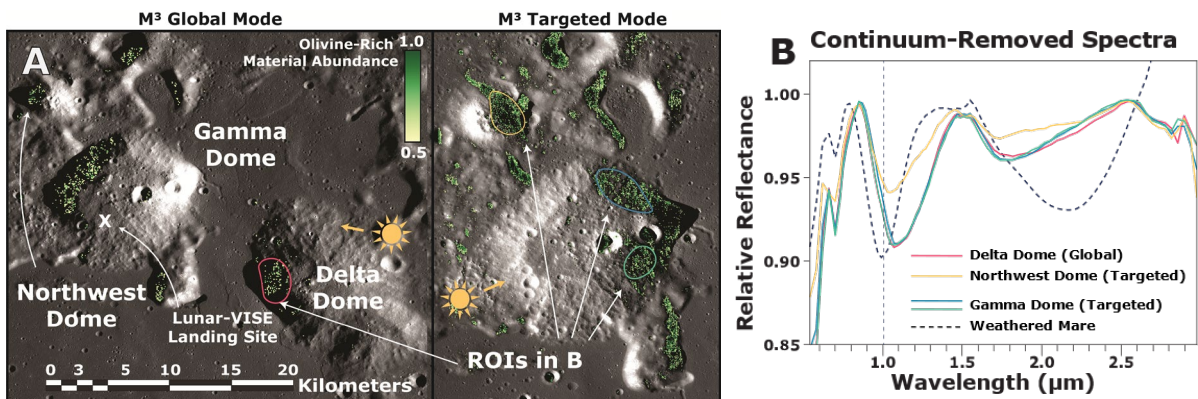


Figure 1: A) Results of Spectral Mixture Analysis (SMA), where the olivine-rich material shown in B was used as an endmember. Regions of olivine-rich material are detected across all three Gruithuisen Domes and are confined to the steep slopes. B) Areally averaged spectra from the regions of interest (ROIs) shown in A. Each ROI shows the distinct long-wavelength shift of the 1 μ m absorption feature with respect to that of the pyroxene absorption seen in the weathered mare. This shift in absorption position is commonly associated with olivine.

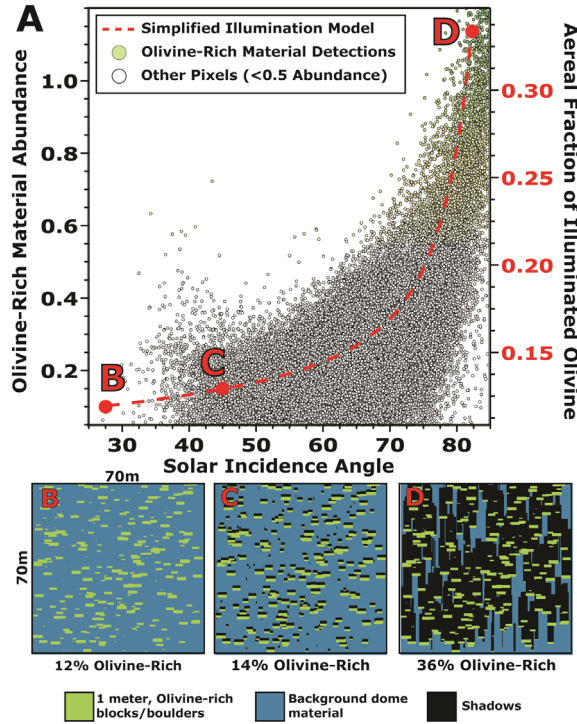


Figure 2: Modeled olivine abundance shows a rough correlation with solar incidence angle. This relationship can be replicated by simply modeling the fractional illuminated area taken up by rectangular positive relief features at increasing solar incidence angles as shown in A, B and C. Our model implies that the olivine-rich material is related to a positive relief feature within the slopes of the domes.

In **Fig 2b-d**, a simplified illumination model shows the shadowing effects that occur when ~1m tall rectangular positive relief features are randomly scattered over the area of a single M^3 pixel. As the solar incidence angle (θ) increases, the fraction of the total illuminated area taken up by the positive relief features (i.e. the olivine-rich material) increases as $\sim \tan(\theta)$. When plotted over the olivine-rich material pixel values (**Fig. 2a**), this relationship or something similar could explain this incidence angle relationship. At low solar incidence angles, the areal fraction of olivine-rich material could be below the detection limit in a single M^3 pixel, but at high solar incidence angles, this areal fraction increases dramatically and could cause a positive detection in M^3 simply due to geometric effects. To confirm this, further work must be done in understanding the spectral components of both the background material and the olivine.

Dome Slope Morphology: Using a variety of visible images taken by LROC NAC at a spatial resolution of ~0.5 m/pixel, we carried out an analysis of the morphology of the steep slopes of the Gruithuisen Domes. The most intriguing result was the identification of rough, elephant hide terrain (EHT) across the slopes of each dome that could either be related to impact processes or downslope movement [12]. **Fig. 3a** shows the same region of EHT at both

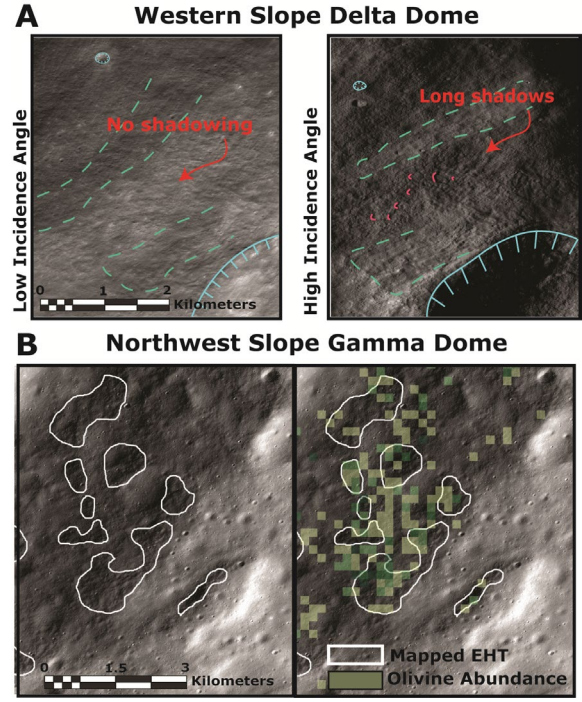


Figure 3: Rough-textured elephant hide terrain (EHT) which may be related to impact processes or downslope movement can be mapped across several localities in the dome slopes. A) Positive-relief features associated with EHT cause compelling shadowing effects at high solar incidence angles. B) Olivine-rich material abundance shows a loose spatial correlation to EHT deposits, which suggests that the olivine-rich material is being exposed via downslope movement.

high and low solar incidence angles and demonstrates that this texture can cause dramatic shadowing effects that are absent in smoother slope material. Preliminary analyses in **Fig. 3b** shows that the spatial distribution of the olivine-rich material is loosely correlated with the mapped EHT. If this relationship holds, it may suggest that the olivine-rich material is being actively exposed by downslope movement.

Acknowledgements: Lunar-VISE is funded through NASA's PRISM2 cooperative agreement number 80NSSC22M0303. *M³ Data Products:* M3T20090418T020644, M3G20090208T194335, M3G20090208T175211, *Kaguya Data Products:* TC2S2A0_02DLF03061_003_0004, MI_MAP_03_N37E319N36E320SC

References: [1] Whitaker, E. A. (1972) *The Moon*, 4, 3-4, 348-355. [2] Kusuma et al. (2012) *Planet Space Sci.*, 67, 1, 46-56. [3] Kumari et al. (2024) *Planet Sci. J.*, 5, 132. [4] Vig et al. (2024) *LPSC*, Abstract #1330. [5] Logan et al. (1973) *JGR*, 78, 23. [6] Glotch et al. (2010) *Science*, 329, 5998, 1510-1513. [7] Jolliff, B.L. (1991) *LPSC*, 21, 101-118. [8] Haggerty et al., (2006) *JGR: Planets* 111, E6. [9] Ryder (1976) *Earth Planet. Sci. Lett.*, 29, 2, 255-268. [10] Donaldson Hanna (2024), *LPSC*, Abstract #2170. [11] Adams and Gillespie (2006) *CUP*. [12] Brown et al. (2023) *DPS. id 207.01*, 55, 8.